Research Article Adv. Mater. Lett. 2016, **7**(2), 136-143 Advanced Materials Letters

www.amlett.com, www.vbripress.com/aml, DOI: 10.5185/amlett.2016.6012

Relaxations in gelatin hydrogels probed by dynamic light scattering

Nitin Kumar[1], **Vinay Kumar**[1, 2], **Jitendra Sharma**[1*]

[1]*School of Physics, Shri Mata Vaishno Devi University, Katra 182320 (J&K), India*
[2]*Department of Physics, University of the Free State, P.O. Box 339, Bloemfontein 9300, South Africa*

[*]Corresponding author. Tel: (+91) 9622220321; E-mail: jitendra.sharma@gmail.com

Received: 06 June 2015, Revised: 20 November 2015 and Accepted: 11 December 2015

ABSTRACT

The relaxation behavior of gelatin aqueous solutions has been investigated by time resolved dynamic light scattering (TRDLS) measurements at different temperatures spanning the entire sol to gel phase transition behavior of the system (i.e. from 5 min to 1440 min after a sudden quench from high temperature sol to low temperature gel state), when the chosen gelatin concentration in water was maintained at 5 % (w/v), well over the overlap threshold. The quantity of interest, structure factor S (q,τ), has been obtained from the experimentally measured autocorrelation function, $g_2(\tau)$, allowing appropriate heterodyne contribution. The nonlinear regression analysis of the obtained scattering profiles (variation of structure factor vs. delay time) exhibited good fits to the function $S(q,\tau) \sim A \exp(-Dq^2\tau) + B \exp(-(\tau/\tau_c)^\beta)$, up to system evolution time of 360 min, whereas the data obtained after 360 min showed appropriate fits to $S(q,\tau) \sim A \exp(-Dq^2\tau) + C\tau^{-\alpha} + B \exp(-(\tau/\tau_c)^\beta)$. The temporal behavior of different fit parameters defining the transient structural network formed in the system has been quantified and analyzed under the purview of well-defined theories. Furthermore, the evolution of particle dynamics from fast to slow and then to almost frozen behavior has been explored through the continuous evaluation of 'Gelation factor (κ)' at different stages of system evolution times during the measurements. Copyright © 2016 VBRI Press.

Keywords: Time resolved dynamic light scattering; gelatin; sol-to-gel transitions; glass transitions; intensity correlation function.

Introduction

Study of the relaxations in disordered (non-equilibrium) systems has since long been amongst the most intriguing problems in condensed matter physics which stipulates in-depth investigations of the underlying physics and related phenomena in complex fluids (such as polymer solutions, gels, glasses and foams, etc.) **[1,2]**. For a polymeric gel system, slow relaxation, in particular, is a consequence of either physical interactions (like dipole-dipole interaction, hydrogen bonding and electrostatic interactions among polymer coils, etc.) or covalent crosslinking (primary forces) i.e., chemical bonding **[3, 4]** and may also be caused by a combination of the two. Usually, physical gels are obtained through a process of gelation which results in the formation of large polymer network caused primarily by the physical entanglement of polymeric chains in the solvent medium **[5, 6]**. Stauffer broadly identified the occurrence of such gelation (sol to gel transitions) to a phenomenon generally understood in terms of percolation (i.e., transition from smaller clusters to giant interconnected network formation) problem **[7]**.

Gelatin, a biopolymer (consisting of ~20 different amino acids linked through peptide bonds), has long been an intriguing material which undergoes physical gelation in hydrophilic solvents, such as water, below a temperature of ~30 °C at a relatively low concentration of the polypeptide chains (about 2 % (w/v)) **[8]**. The thermodynamics of which has been explained by Eldridge and Ferry in terms of Van't Hoff equation **[9]**. Investigations on both physically as well as chemically crosslinked gelatin gels have been carried out to elucidate both the structure **[10-12]** and dynamics **[8-12]** of such sol to gel transitions **[13-15]**. In a related study, Ren and Sorensen **[16, 17]** observed drastic changes in the intensity correlation function (*ICF*) at the gelation threshold, wherein the slow mode of intensity-time correlation functions diverged and an additional power law behavior appeared at the gelation threshold hence clearly indicting that such structural transitions from sol to gel states may be construed as an ergodic-to-nonergodic transitions **[18]**.

Recently, many other workers have also reported that gel threshold of a system is a point at which at least four characteristic variations occurs: (a) drastic increase in the scattered intensity, (b) depression in the initial amplitude of *ICF*, and (c) power law behavior in *ICF* accompanied by (d) broadening in decay time distribution function **[19-21]**. These changes broadly signify the evolution of a system from ergodic (sol) to non-ergodic (gel) phase. The observations of these characteristic changes in such systems are often identified with manifestation of gel and gel-like (glass) system behavior **[22]**. Hence, sol to gel transitions is very much an illustration of α– and β– type relaxations in glassy systems as predicted by mode coupling theory (*MCT)* **[23]**. As per the predictions of *MCT* and also proved by experiments a power-law β relaxation to a nonergodic background exists below the glass transition temperature **[24-26]**.

Light scattering is an effective tool to probe the relaxation behavior of gel systems. Recently, the relaxations in polymeric gels have been studied experimentally by many workers by means of time resolved dynamic light scattering *(TRDLS)* **[21, 22, 27]**. *TRDLS* is a tool in which variation of scattered intensity *vs.* delay time is recorded at a fixed scattering angle, which over the time has emerged as a well-known technique for characterizing relaxations in polymer gels **[25, 28]**.

In this work, we report the study of time evolution of relaxations (spanning the entire sol to gel phase transitions) in aqueous solution of gelatin (above overlap concentration) which is quenched suddenly to a temperature below the gelation threshold, probed by the commonly used-TRDLS' techniques. The contribution of heterodyne extent, which is often neglected in the TRDLS data analysis, has been accounted for in estimating the dynamic structure factor, $S(q,\tau)$ both in the sol and gel states of the system. The objective was to interpret the temporal behavior of different fit parameters under the purview of well-defined theories capable to map this path of transition and identify those dynamical signatures and similarities, if any, that are shared amongst the two most intriguing but theoretically identified similar phenomena of the sol to gel transitions and glass transitions, in physics. We also identified an important parameter called the "Gelation factor" to quantify the extent of slowing down of dynamics i.e., presence of frozen component at different stages of the evolution of system.

Experimental

Materials

The high purity gelatin (bovine origin) was purchased from M/S Loba Chemie (Indo-Astranal Co. India) and was used without further purification. And this sample preparation was free from any *E. coli* and liquefier presence. The gelatin sample used had a narrow molecular weight distribution with M_w peak at about 1.5×10^5.

Preparation

For sample preparation gelatin was dissolved in sodium phosphate buffer (Na_2HPO_4 + $NaH_2PO_4.2H_2O$), followed by heat treatment for about 60 min at 55 °C to remove the effects of sample history, if any, present in the solution. The obtained solutions were then ultra-centrifuged for about 60 min at about 5500 rpm to eliminate dust particles. The obtained solutions looked transparent with light-yellow hue and were used directly for *TRDLS* experimental measurements without processing further. Before *TRDLS* measurements, the solutions were allowed to equilibrate for nearly 10-15 hours at room temperature as the aliquot settled into homogeneous gels.

Scattering set up

The TRDLS studies were carried out on a home-made scattering set up made of a goniometer and a sample chamber equipped fitted with suitable temperature sensors (with a precision of ± 0.1°C). A Diode pumped solid-state laser (Adlas, Germany) operating at a wavelength of 514 nm with power output of 50 mW was used for excitation. The intensity correlation data from the scattered light was measured by photon counter and a digital auto correlator (BI-9000 AT Brookhaven Instrument Corporation, USA). The counting rate in the range of 10^4-10^5 counts per second was fixed for improved data statistics.

Scattering measurements

Before any measurement, the scattering set up was calibrated by using a dilute suspension of standard polystyrene latex solution. To perform scattering measurements, the physically entangled network of gelatin gels were heated again to ca. 60 °C to reproduce hot gelatin solutions, before performing the temperature quench experiment. The so obtained solutions were loaded in the quartz scattering cells to obtain the intensity correlation functions (ICFs) at regular intervals of time (from 5 min to 24 hours) in the local ambience 20±0.1 (°C). The measurements were carried out at fixed scattering angle $\theta = 90°$.

Analysis of the DLS data

DLS is an effective tool for studying the various relaxation processes occurring in glassy systems **[29]**. Such tools have successfully been utilized for the studying system dynamics in macromolecular gels as well **[22, 30]**. The apparent measure of system dynamics in such systems obtained from DLS experiments is the normalized intensity-time autocorrelation function given by

$$g_2(\tau) = \frac{\langle I(q,0)I(q,\tau)\rangle}{\langle I(q,0)\rangle^2} \qquad (1)$$

where, $g_2(\tau)$ is the intensity correlation function, $I(q,\tau)$ being the scattered intensity at delay time τ, and $q = \left(\frac{4\pi n}{\lambda}\right)\sin\left(\frac{\theta}{2}\right)$, the scattering wave vector.

The so obtained normalized autocorrelation function $g_2(\tau)$ is related to the dynamic structure factor $S(q,\tau)$ through the relation **[31]**:

$$g_2(\tau) = 1 + \beta'\{2Y(1-Y)S(q,\tau) + Y^2|S(q,\tau)|^2\} \qquad (2)$$

Here, β' is the coherence area factor and its value here is taken unity for simplicity (being a scaling factor only), Y ($0 \le Y \le 1$) being a parameter which provides the measure for the extent of heterodyne contribution (through σ^2 as defined in eq. (3) below present in the obtained $g_2(\tau)$ data. In the sol state, $Y = 1$ this simply implies that the system dynamics can be attributed to purely thermally fluctuating components, only. Thus the Siegert relationship $g_2(\tau) = 1 + \beta'|S(q,\tau)|^2$ is appropriate to determine structure factor data $S(q,\tau)$ in the sol state. However, in the gel state $Y < 1$, and the contribution from the component

$2Y(1-Y)$ dominates $g_2(\tau)$ and therefore needs to be accounted for. We evaluated the values of Y by using the approach used by Asai *et al.* **[27]** as:

$$\sigma^2 = Y(2-Y) \qquad (3)$$

Here, σ^2 is the initial amplitude of $g_2(\tau)$ (when, $S(q,\tau)=1$). The variation of Y with time has been depicted in **Fig. 1**.

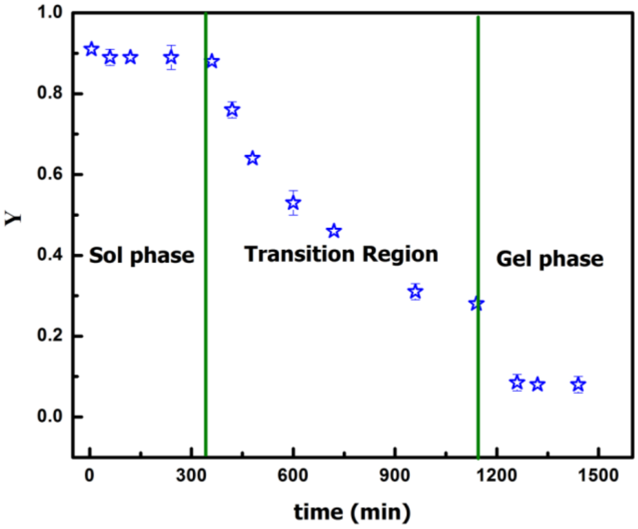

Fig. 1. Plot of heterodyne parameter (Y) as a function of evolution time.

For sol state, we obtained $Y \sim 0.89$; thus we can neglected the contribution of $2Y(1-Y)$ for the evaluation of $S(q,\tau)$ and so,

$$S(q,\tau) = \left\{\frac{[g_2(\tau)-1]}{\beta'}\right\}^{1/2} \qquad (4)$$

We examined the time resolved dynamic light scattering (TRDLS) measurement parameters for a system of 5 % (w/v) gelatin aqueous solutions as the system evolved from a high temperature sol to ambient gel state caused by a sudden temperature-quench from very high to ambient room temperature conditions. The entire pathway spanning the sol to gel state transition has been captured through measurements of the dynamic structure factor, $S(q,\tau)$ data. **Fig. 1** depicts the variation of heterodyne parameter during such transitions wherein a continuous decrease in Y (as defined in eq. (2) and eq. (3)) beyond the evolution time of *Et* ~ 360 min is observed which continues up to an evolution time of *Et* ~ 1140 min. And this is identified as the transient sol to gel transition region of the system, for which the term $2Y(1-Y)$ dominated in $g_2(\tau)$ and hence been accounted for accordingly thus, allowing the evaluation of $S(q,\tau)$ directly from eq. (2). Beyond 1140 minutes of evolution time (*Et*), the parameter *Y* saturates to *~0.08* indicating that the system has entered into a persistent gel state (wherein the parameter Y^2 is very small and therefore can be neglected). As the pre-factor of $S(q,\tau)$ in eq. (2) now becomes roughly 20 times higher in comparison with the prefactor $|S(q,\tau)|^2$. We neglected the contribution of the second term for the evaluation of $S(q,\tau)$ to re-write eq. (2) as:

$$S(q,\tau) = \frac{[g_2(\tau)-1]}{\beta'[2Y(1-Y)]} \qquad (5)$$

Fig. 2 shows the subsequent evolution of the dynamic structure factor $S(q,\tau)$ data immediately after the temperature quench – when the settled gels (of gelatin in water) homogenized as high temperature at (~ 55 ^{0}C) were suddenly dipped in a water bath (i.e., quenched to room temperature, which at the time of experiments was below the known gelation temperature of ~28 ^{0}C). Signature of changes in system dynamics were noted through the observed change in overall amplitude of $S(q,\tau)$ at different evolution times (following the quench). $S(q,\tau)$ exhibited the maximum amplitude during the initial phase of system evolution time up to ~360 min (stage - I) after which an abrupt and continuous decrease in the amplitude occurred up to the time ~1140 min (stage - II) and finally becomes almost frozen (constant) for evolution times after 1140 min (stage - III). Stage - I is identified as the fluid-like ergodic sol state, stage – II represented the transition phase (fluid-like sol to solid-like gel). And, the finally (stage - III) the formation of gels is complete when is dynamics gets completely frozen, a reflection of non-ergodicity in the system.

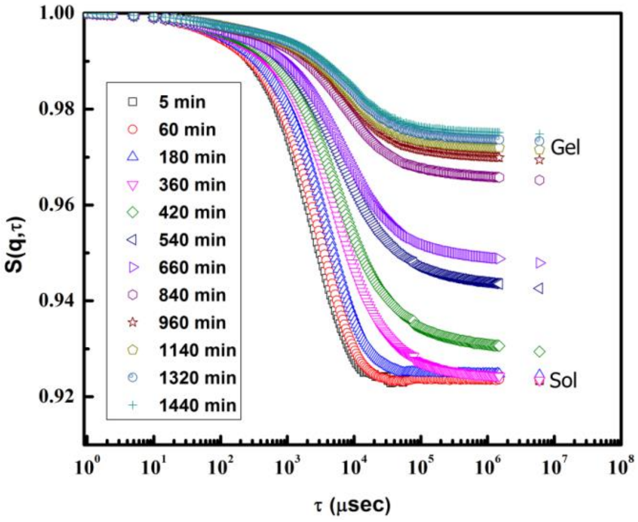

Fig. 2. Dynamic structure factor S(q,τ) as a function of delay time (τ) at different but regular intervals of time (t) spanning the entire sol to gel phase transition occurring in the system as the system is quenched from a high temperature to ambient conditions of room temperature.

Further, the extent of freezing component present in a system undergoing ergodic (sol) to non-ergodic (gel) transitions, has been monitored through the continuous evaluation of parameter termed 'Gelation factor (κ)' and obtained empirically from the dynamic structure factor data as follows;

$$\kappa = 1 - \left|\frac{S_{Et}(q,0) - S_{Et}(q,\infty)}{S_{Et=0}(q,0) - S_{Et=0}(q,\infty)}\right| \qquad (6)$$

where, *'Et'* is the evolution time after the temperature quench. The variation of gelation factor (κ) as function of evolution time is depicted in **Fig. 3**, which clearly indicates that the system undergoes transitions from initial ergodic to final non-ergodic state via three different stages, namely; the initial sol state, the intermittent transition region or the gelation region and the final gel state during the entire evolution process. The parameter κ $(0 \leq \kappa \leq 1)$ is defined such that $\kappa \cong 0$ in the completely sol state (indicating no entanglement/crosslinking among polymer coils and absence of freezing component) and approaches $\kappa \leq 1$ for gel state (indicating maximum entanglement/crosslinking among polymer coils and higher contribution of the freezing component). We obtained $\kappa \sim 0.1$ for the sol state while a value of $\kappa \sim 0.66$ was recorded in the gel state.

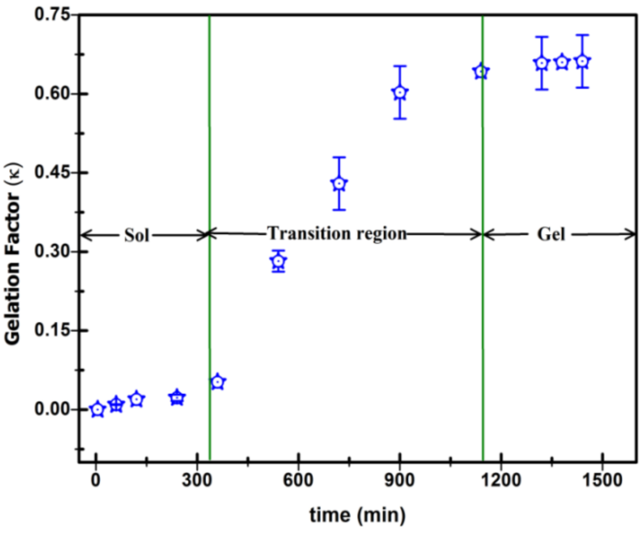

Fig. 3. Variation of Gelation factor (κ) as a function of time.

Results and discussion

A drastic change in the overall amplitude of $S(q,\tau)$ (*see* **Fig. 2**) beyond 360 min of evolution time has been identified as the onset of gelation i.e., the gelation threshold time (t_0) as has been argued by other researchers as well **[2, 32, 33]** and the magnitude of such decrease in amplitude during the transitions is indicative of the extent of network formation due to entanglement of chains **[28, 34]**. However, it is not easy to estimate or pinpoint an exact value of the gelation threshold or onset of gelation based simply on the visual examination of the observed changes in amplitude of $S(q,\tau)$ alone. Therefore, we also studied the underlying changes in the relaxation behavior of the system obtained directly from the rapid analysis of $S(q,\tau)$ data, which involved the determination of physical parameters such as; diffusion coefficient (D), hydrodynamic radius (R_H), relaxation width, and characteristic relaxation time, etc. The intensity correlation profiles revealed two modes of relaxations in the sol state $(t \leq 360\ \text{min})$ interpreted as; the fast mode at shorter delay times (the so-called incipient gel mode) and the slow mode at longer delay times associated with the diffusion of finite gelatin clusters. With time, these finite clusters grow in size to make a giant inter-connected infinite network of chains. As the system enters gels phase i.e., the transformation of transient clusters of chains into giant network of gels, the intensity correlation profiles exhibited three modes of relaxations identified as the fast mode at shorter delay times; a power law behavior at intermediate times which crosses over to stretched exponential behavior i.e., slower mode relaxation or at longer delay times.

For evaluation of relevant parameters structure factor data $S(q,\tau)$ data for the sol state are fitted to equation of the form;

$$S(q,\tau) = Aexp(-Dq^2\tau) + Bexp\left(-\left(\frac{\tau}{\tau_c}\right)^{\beta}\right) \qquad (7)$$

And for gel state, the equation of the following form has been used:

$$S(q,\tau) = Aexp(-Dq^2\tau) + C\tau^{-\alpha} + Bexp\left(-\left(\frac{\tau}{\tau_c}\right)^{\beta}\right) \qquad (8)$$

Typical fits for fast and slow relaxation modes in the sol state and to fast, intermediate and slow relaxation modes in gel state have been depicted in **Fig. 4(a) and Fig. 4(b)** respectively.

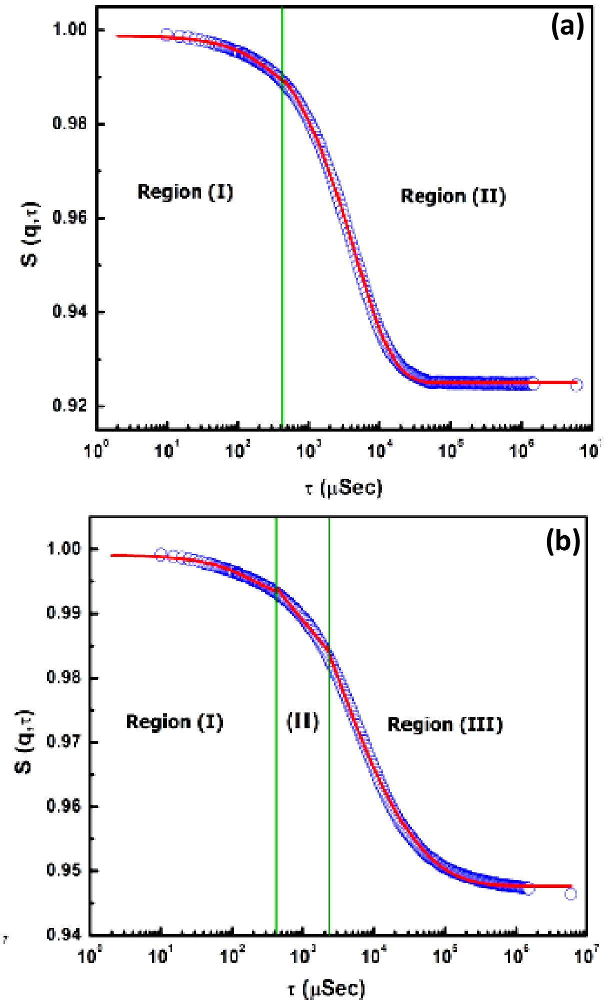

Fig. 4. (a) Fitting of the S (q, τ) data at evlution time of 180 min to eq. (7). Region (I) and (II) represents the exponential and stretched exponential fits, respectively (b) Fitting of the S (q,τ) data at 600 min to eq. (8). Region (I), (II) and (III) represent the exponential, power law and stretched exponential fits, respectively.

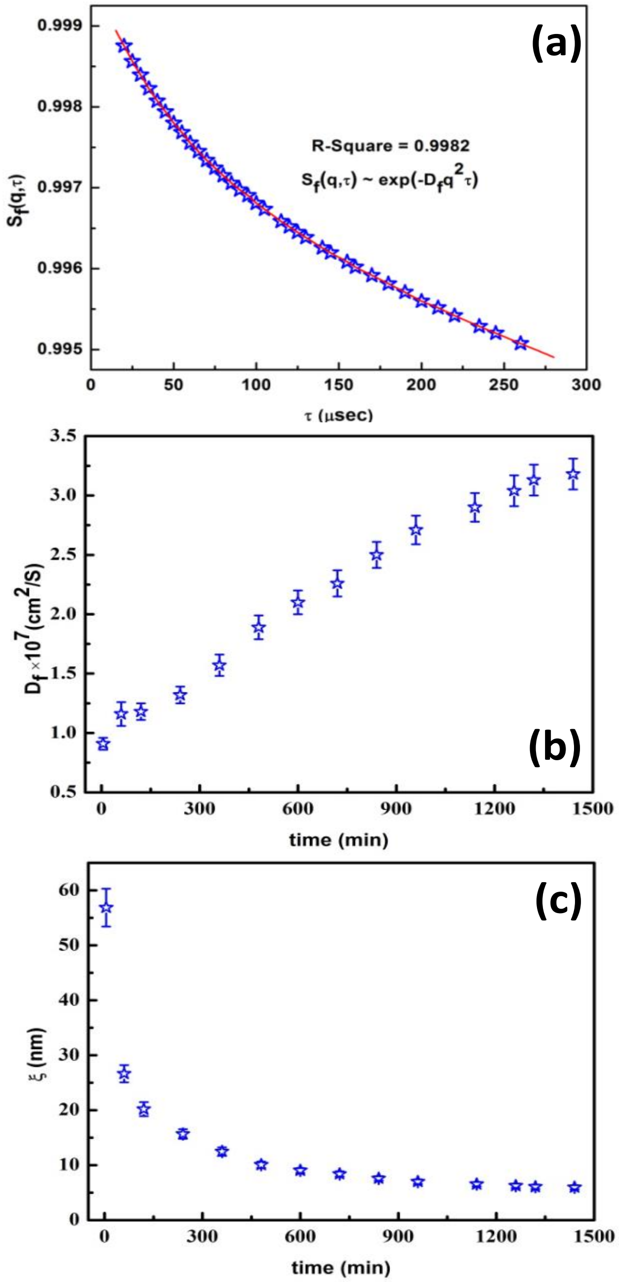

Fig. 5. (a) Initial or fast decay regime of the dynamic structure factor $S(q,\tau)$ for 720 min and its fitting (red solid line) to $S_f(q,\tau) \sim \exp(-D_f q^2 \tau)$ (b) Variation of fast mode diffusion coefficient (D_f) as a function of evolution time. (c) Plot of the mesh size ξ (fast mode) as a function of time (t). The solid red line represents the fitting curve.

Fast mode relaxation

The data obtained up to the delay time of $\tau \leq 300\ \mu sec$ at all evolution times were fitted successfully to $S(q,\tau) \sim \exp(-\Gamma_f \tau) \sim \exp(-D_f q^2 \tau)$, representing the fast mode of relaxation. **Fig. 5(a)** shows a typical fit for the fast mode of relaxation at an evolution time of 720 min. As $\Gamma_f = D_f q^2$ gives the estimation of the rate of relaxation, the fast mode diffusion coefficient, D_f, was evaluated from $D_f = \frac{\Gamma_f}{q^2}$. The variation of D_f *vs.* evolution time has an almost exponential growth behavior (*see* **Fig. 5(b)**).

For a sol state, in which polymer coils maintain their individual identities, the magnitude of the hydrodynamic radius R_H can be evaluated through well-known Stokes-Einstein relation **[35]**;

$$R_H = \frac{k_B T}{6\pi\eta_0 D} \tag{9}$$

where, k_B being the Boltzmann's constant, T the absolute temperature, and η_0 represents the viscosity of the solvent.

However, for in the gel state, the rapid entanglement of chains results in the overall growth of the network dimensions. At this stage the scattering window does not just include the individual polymer chains, but the entire sub-region present in the network (i.e. a component of gelled structure) having characteristic size dimensions (ξ) termed as mesh size **[22]**. The replacement of R_H by ξ, in eq. (9) thus provides a measure of the relevant length scale;

$$\xi = \frac{k_B T}{6\pi\eta_0 D} \tag{10}$$

The measured values of mesh size have been plotted as a function of evolution time, indicating strong time dependence (*see* **Fig. 5(c)**). As the system undergoes transition from sol to gel state, the associated value of mesh size ξ, decreases up to evolution time of ~ 360 min and beyond it becomes almost constant. This point at which ξ attains a constant value may be assumed to be the beginning of gelation or gelation threshold.

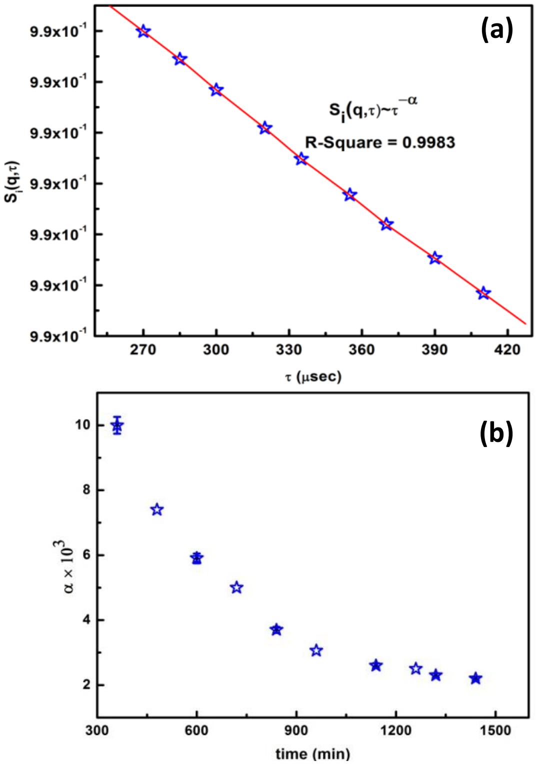

Fig. 6. (a) Intermediate or power law relaxation regime of the dynamic structure factor data for the system evolution time of 720 min and its fitting to $S_i(q,\tau) \sim \tau^{-\alpha}$ (red solid line). (b) Plot of the power exponent (α) as a function of system evolution time.

Intermediate power law relaxation

For the DLS data (scattering profile) in the intermediate delay time, the measured $S(q,\tau)$ data were fitted to a pwer law behavior, $S(q,\tau) \sim \tau^{-\alpha}$ (*see* **Fig. 6(a)**) where the exponential fitting was not adequate.

This mode of relaxation appeared beyond system evolution time of 360 min, when the system begins to make a transition from sol to gel state. The appearance of the power law-relaxation signifies a non-ergodic background in gelatin gels and this point may be taken as the gelation threshold **[20, 22, 35]** of the system. Such systems generally restore ergodicity by undergoing a change from a power law to stretched exponential behavior in a completely sol state. Thus, the recorded time-resolved dynamic structure factor data clearly exhibited a transition from ergodic sol (state) to non-ergodic gel state of the system. The variation of power law exponent (α) as a function of time has been shown in **Fig. 6 (b).**

Slow mode relaxation

Fig. 7(a) shows a typical fit of dynamic structure factor $S(q,\tau)$ data to the stretched exponential function, $S_s(q,\tau) \sim exp\left(-\left(\frac{\tau}{\tau_c}\right)^{\beta}\right)$. Excellent fit to this mode was observed for both the sol and gel states which yielded fascinating factual consequences. The parameter τ_c, being the characteristic relaxation time, signifies component of the relaxation time distribution in which the majority of relaxation phenomenon occurs and the parameter $'\beta'$ is simply the width of the distribution having the range, $0 < \beta < 1$.

For $\beta = 1$, a simple dynamic process with single exponential decay of fluctuations is obtained for the diffusion of a typical nanoparticle (or say a coil polymer coil) in a dilute solution (gelatin in water). As β deviates from unity towards zero, a more complex dynamical behavior and a wider distribution of relaxations in the system as the one manifested in the present case is observed. One can also assume β as a measure of the extent of “heterogeneity” in the system.

The variation of β versus evolution time is depicted in **Fig. 7(b)**. With a maxima at initial evolution times, a uniform decrease in β occurs up to system evolution time of ~ 360 min, which is the gelation threshold. This is due to the formation of transient structural entities caused by overlapping of the high molecular weight gelatin coils during the initial stages of entanglement. These coils are capable of attaining different kinds of entanglements due to wider relaxation time distribution as envisaged in the case of stress relaxation of polystyrene in the rubbery region **[36]**. Further, a drastic change in β value i.e., a sharp and sudden dip observed around 360 min of system evolution time clearly indicates a sol to gel phase transitions in the system. Similar behavior has also been observed by Morais *et al.* from covalent crosslinking of chitosan solutions with glutaraldehyde as cross linker **[2]**. The β obtained for both (sol and gel) states were fitted to $\beta(t) = a_0 + a_1 t + a_2 t^2$, shown in **Fig. 7(b)**. In sol state the fitted parameters were $a_0 = (873.07 \pm 9.27) \times 10^{-3}$,
$a_1 = (-47.7 \pm 1.82) \times 10^{-5}$
and $a_2 = (-33.7 \pm 1.72) \times 10^{-7}$ whereas for gel state $a_0 = (15.81 \pm 3.0) \times 10^{-2}$,
$a_1 = (24.04 \pm 7.92) \times 10^{-5}$,
and $a_2 = (-6.62 \pm 3.45) \times 10^{-8}$. The mean value of β obtained was 0.81 ± 0.06 for the sol and 0.39 ± 0.02 in the gel state.

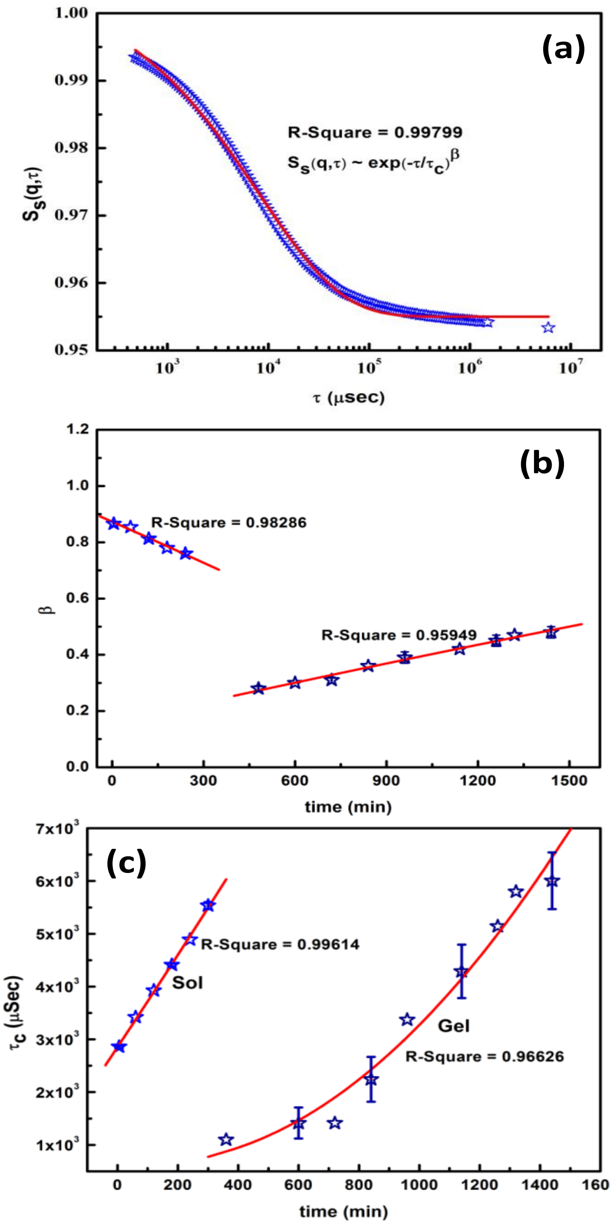

Fig. 7. (a) Slow mode or the stretched exponential regime of the dynamic structure factor $S(q,\tau)$ for evolution time of 720 min and its fitting to $S_s(q,\tau) \sim exp\left(-\left(\frac{\tau}{\tau_c}\right)^{\beta}\right)$ (solid red line). (b) Variation of the width exponent (β) as a function of evolution time, in the sol and gel states. The red lines represent the curves fitted to $\beta(t) = a_0 + a_1 t + a_2 t^2$. (c) Variation of the relaxation time (τ_c), as a function of evolution time. The red lines represent the curves fitted to $\tau_c(t) = b_0 + b_1 t + b_2 t^2$.

Fig. 7(c) shows the variation of relaxation time (τ_c) *vs.* evolution time. It implies that the characteristic relaxation time (τ_c) after an initial increase (linear) drops suddenly at evolution time of ~ 360 min, the gelation threshold, which marks the beginning of the entanglements for the incipient gels. After reaching the gelation threshold, τ_c increases again with a $\tau_c(t) = b_0 + b_1 t + b_2 t^2$ dependence of the relaxation time (τ_c) on the system evolution time. The obtained fit parameters are $b_0 = 689.54$, $b_1 = -0.64$ and $b_2 = 3.2 \times 10^{-3}$ in the gel state. The divergence observed in the relaxation time is typical of a gelling system.

Power law and stretched exponential behavior

At shorter evolution times, up to 360 min the system remains in sol state. As system equilibrates further with time beyond the gelation threshold, it results in the formation of finite overlapping clusters which matures into a well-developed network of chains, the gels. The decay of intensity correlation exhibits an extended tail with an associated slower relaxation time. Beyond this time (360 min) the rate of this decay becomes slower resulting in the growth of tail at higher delay times. The $S(q,\tau)$ data at intermediate delay times shows very good fit to power law behaviour. Moreover the values obtained for relaxation time, τ_c, increases gradually towards complete volume-filling with overlapping clusters prior to the formation of a fully grown infinite network of gels. Thus, it may be concluded that the power law behavior marks the beginning for setting-in of non-ergodicity in the system. For the slow mode, our experimentally measured β values are 0.81 and 0.39 for sol and gel states, respectively. The main cause of the power law and stretched exponential behavior in terms of dynamics have frequently been explained in the context of the well-known theories based on the spring and bead model either with or without hydrodynamic interactions. A revelant reptation model takes movement of topologically restricted chains into account to assume that the chains move in a restricted tube along its length. Using the Gaussian chain proposition, the dynamic structure factor $S(q,\tau)$ for the Rouse, Zimm, and Reptation models of relaxation can be written as **[37];**

$$S(q,\tau) = S(q,0)exp\left(-\left(\frac{\tau}{\tau_c}\right)^m\right) \tag{11}$$

With

$$m = \begin{cases} \frac{1}{2}; & \text{Rouse model} \\ \frac{2}{3}; & \text{Zimm model} \\ \frac{1}{4}; & \text{Reptation model} \end{cases} \tag{12}$$

Thus, for stretched exponential regime, i.e., $S(q,\tau) \sim exp(-\tau/\tau_c)^\beta$, $\beta = {}^1\!/_2$ for Rouse type dynamics and $\beta = {}^2\!/_3$ for Zimm type dynamics.

Ren *et al*. obtained $\beta = 0.81$ for sol state and $\beta = 0.65$ for the gel state **[16, 17]**. For gelatin-SDS complexes $\beta = 0.85$ has been reported for both the sol and gel states of this biopolymer **[38]**. The value of $\beta = 0.86$ in the sol state and $\beta = 0.65$ were obtained for chemically crosslinked gelatin gels **[9]**. We obtained the mean value of $\beta = 0.81$ for the sol state, which implies a dynamical behavior close to Zimm-type relaxation whereas $\beta = 0.39$ for the gel state. The β value obtained in a gel state show that neither the Rouse model nor the Reptation model is fully appropriate to describe the observed relaxation behavior and indicates that the associated dynamics manifests a behavior that only lies in-between the Reptation and Rouse-type relaxation. Thus, in the gel state, the system follows a dynamical behavior wherein the movement of chains is largely affected by the presence of other chains as topological constraints offered by the entanglements of long polymer chains. Hence, the overall dynamics is akin to a rather slower reptation-like movement of chains along a topologically constrained tube.

Table 1. Values of the heterodyne contribution factor (Y), fast diffusion coefficient (D_f), relaxation width (β), relaxation time (τ_c), and gelation factor (κ) obtained for different intervals of time.

t (min)	*Y*	$D_f \times 10^{-7}$ (cm²/S)	β	τ_c (µSec)	*K*
5	0.91 ± 0.03	0.91 ± 0.05	0.86 ± 0.08	2860 ± 24	0
60	0.89 ± 0.02	1.16 ± 0.10	0.85 ± 0.03	3421 ± 13	0.094 ± 0.005
120	0.89 ± 0.02	1.18 ± 0.07	0.81 ± 0.05	3927 ± 23	0.019 ± 0.006
240	0.89 ± 0.03	1.32 ± 0.07	0.76 ± 0.06	4889± 39	0.02 ± 0.006
360	0.88 ± 0.02	1.57 ± 0.09	0.34 ± 0.01	1096 ± 208	0.05 ± 0.005
480	0.64 ± 0.03	1.89 ± 0.10	0.28 ± 0.01	754 ± 199	0.16 ± 0.05
600	0.53 ± 0.01	2.10 ± 0.10	0.30 ± 0.01	1415 ± 295	0.29 ± 0.06
720	0.46 ± 0.02	2.26 ± 0.11	0.31 ± 0.01	1412 ± 326	0.43 ± 0.05
840	0.37 ± 0.03	2.50 ± 0.11	0.36 ± 0.02	2243 ± 424	0.51 ± 0.05
960	0.31 ± 0.02	2.71 ± 0.12	0.39 ± 0.02	3372 ± 486	0.60 ± 0.06
1140	0.28 ± 0.01	2.90 ± 0.12	0.42 ± 0.02	4288 ± 506	0.64 ± 0.06
1260	0.09 ± 0.02	3.04 ± 0.13	0.45 ± 0.02	5143 ± 517	0.65 ± 0.05
1320	0.08 ± 0.02	3.13 ± 0.13	0.47 ± 0.02	5798 ± 537	0.66 ± 0.05
1440	0.08 ± 0.02	3.18 ± 0.13	0.48 ± 0.02	6004 ± 526	0.66 ± 0.05

Conclusion

Relaxations in gelatin aqueous solutions above overlap concentration have been studied by TRDLS measurements. The system at high temperature was quenched suddenly to ambient room temperature (well below the critical gelation temperature) where it was allowed to thaw/equilibrate and evolve structurally with time. The process of different transitions were quantified from the obtained structure factor data and analyzed under the purview of well-defined theories to predict the transient structures formed during transitions. The dynamic structure factor, S(q,τ) data exhibited two different regimes of relaxations in the entire region spanning the sol to gel transitions. As such the evolution pathway was marked by the presence of two different regimes of relaxations – one up to an evolution time of ~ 360 min with two different kinds of relaxation components having an initial single exponential (fast mode) and a stretched exponential (slow mode) decay at larger delay times of the correlation function; and the other recorded beyond evolution time of 360 min with three different kinds of relaxation components comprising an initial single exponential, the intermediate power law, and stretched exponential tail in the correlation functions. As signature of such transitions the relaxation time distribution (from the stretched exponential decay) width parameter β were also estimated. The stretched exponential exponent (β) obtained in the sol and gel phase were 0.81±0.06 and 0.39 ±0.02, respectively. In addition, the observed drastic decrease in the amplitude of S(q,τ), appearance of power law behavior, a sharp transition in the magnitude of the width exponent (β) of relaxation times (τ_c) coupled with a jump in the gelation factor (κ) occurring near evolution time of 360 min, implied it to be the gelation threshold. The appearance of power law behavior beyond 360 min signified a transition from ergodic sol to non-ergodic gel state in the system.

In the gel state, the power law relaxations to nonergodic background observed here are analogous to the ones (β and α type) associated with systems with glassy dynamics described by the mode coupling theory **[23]**.

Reference

1. Cipelletti, L.; Ramos, L. *Curr. Opin. Colloid Interface Sci.* **2002**, *7*, 228.
   DOI: 10.1016/S1359-0294(02)00051-1
2. de Morais, W. A.; Pereira, M. R.; Fonseca, J. L. C. *Carbohydr Polym.* **2012**, *87*, 2376.
   DOI: 10.1016/j.carbpol.2011.11.002
3. Bordi, F.; Paradossi, G.; Rinaldi, C.; Ruzicka, B. *Physica A: Statistical Mechanics and its Applications* **2002**, *304*, 119.
   DOI: 10.1016/S0378-4371(01)00537-4
4. Starodoubtsev, S. G.; Kidoaki, S.; Yoshikawa, K. *Biomacromolecules* **2002**, *4*, 32.
   DOI: 10.1021/bm025583e
5. Carn, F.; Djabourov, M.; Coradin, T.; Livage, J.; Steunou, N. *J. Phys. Chem. B* **2008**, *112*, 12596.
   DOI: 10.1021/jp802146g
6. Cheng, Y. H.; Yang, S. H.; Lin, F. H. *Biomaterials* **2011**, *32*, 6953.
   DOI: 10.1016/j
7. Stauffer, D. *J. Chem. Soc., Faraday Trans. 2* **1976**, *72*, 1354.
   DOI: 10.1039/F29767201354
8. Sharma, J.; Bohidar, H. B. *Colloid. Polym. Sci.* **2000**, *278*, 15, and references therein.
   DOI: 10.1007/s003960050003
9. Eldridge, B. J.; Ferry, J. D. *J. Phys. Chem.* **1954**, *58*, 992.
   DOI: 10.1021/j150521a013
10. Boedtkaer, H.; Doty, P. *J. Phys. Chem.* **1954**, *58*, 968.
    DOI: 10.1021/j150521a010
11. Sharma, J.; Bohidar, H. B. *Eur. Polym. J.* **2000**, *36*, 1409.
    DOI: 10.1016/S0014-3057(99)00206-2
12. Djabourov, M.; Leblond, J.; Papon, P. *J. Phys. France* **1988**, *49*, 333.
    DOI: 10.1051/jphys:01988004902033300
13. Bohidar, H. B.; Jena, S. S. *J Chem. Phys.* **1993**, 98, 3568.
    DOI: 10.1063/1.464080
14. Bohidar H. B.; Jena S. S. *J Chem. Phys.* **1993**, *98*, 8970.
    DOI: 10.1063/1.464456
15. Bohidar, H. B.; Jena S. S. *J Chem Phys* **1994**, *100*, 6888.
    DOI: 10.1063/1.467004
16. Ren, S. Z.; Shi, W. F.; Zhang, W. B.; Sorensen, C. M. *Phys. Rev. A*, **1992**, *45*, 2416.
    DOI: 10.1103/PhysRevA.45.2416
17. Ren, S. Z., Sorensen, C. M. *Phys. Rev. Lett.* **1993**, *70*, 1727.
    DOI: 10.1103/PhysRevLett.70.1727
18. Pusey, P. N.; Van Megen W. *Physica A* **1989**, *157*, 705.
    DOI: 10.1016/0378-4371(89)90063-0
19. Shibayama, M.; Takata, S.; Norisuye, T. *Physica A* **1988**, *249*, 245.
    DOI: 1016/S0378-4371(97)00472-X
20. Shibayama, M.; Norisuye, T. *Bull. Chem. Soc. Jpn.* **2002**, *75*, 641.
    DOI: 10.1246/bcsj.75.641
21. Okamoto, M.; Norisuye, T.; Shibayama, M. *Macromolecules* **2001**, *34*, 8496.
    DOI: 10.1021/ma010734b
22. Shibayama, M. *Bull. Chem. Soc. Jpn.* **2006**, *79*, 1799.
    DOI: 10.1246/bcsj.79.1799
23. Johari, G. P.; Goldstein, M. *J. Chem. Phys.* **1970**, *53*, 2372.
    DOI: 10.1063/1.1674335
24. Mezei, F.; Knaak, W.; Farago, B. *Phys. Rev. Lett.* **1987**, *58*, 571.
    DOI: 10.1103/PhysRevLett.58.571
25. Richter, D.; Frick, B.; Farago, B. *Phys. Rev. Lett.* **1988**, *61*, 2465
    DOI: 0.1103/PhysRevLett.61.2465
26. Tao, N. J.; Li, G.; Cummins, H. Z. *Phys. Rev. Lett.* **1991**, *66*, 1334.
    DOI: 10.1103/PhysRevLett.66.1334
27. Asai, H.; Nishi, K.; Hiroi, T.; Fujii, K.; Sakai, T.; Shibayama, M. *Polymer* **2013**, *54*, 1160.
    DOI: 10.1016/j.polymer.2012.12.053
28. Matsunaga, T.; Shibayama, M. *Phys. Rev. E* **2007**, *76*, 030401(R).
    DOI: 10.1103/PhysRevE.76.030401
29. Degiorgio, V.; Piazza, R. *Current Opinion in Colloid & Interface Science*, **1996**, *1*, 11.
    DOI: 10.1016/S1359-0294(96)80038-0
30. Shibayama, M. *Macromolecular Chemistry and Physics* **1998**, *199*, 1.
    DOI:10.1002/(SICI)1521-3935(19980101)199:1<1::AID-MACP1>3.0.CO;2-M
31. Joosten J. G. H.; McCarthy J. L.; Pusey P. N. *Macromolecules* **1991**, *24*, 6690.
    DOI: 10.1021/ma00025a021
32. Takata, S.; Norisuye, T.; Tanaka, N. Shibayama, M.; *Macromolecules* **2000**, *33*, 5470.
    DOI: 10.1021/ma0003295
33. Yoshida, K.; Yamaguchi, T.; Osaka, N.; Endo, H. Shibayama, M. *Physical Chemistry Chemical Physics* **2010**, *12*, 3260.
    DOI: 10.1039/B920187D
34. Joosten, J. G. H.; Geladé, E. T. F.; Pusey, P. N. *Physical Review A* **1990**, *42*, 2161.
    DOI: 10.1103/PhysRevA.42.2161
35. Shibayama, M.; Takata, S.; Norisuye, T. *Physica A: : Statistical Mechanics and its Applications* **1998**, *249*, 245.
    DOI: 10.1016/S0378-4371(97)00472-X
36. Knoff, W. F.; Hopkins, I. L.; Tobolsky, A. V. *Macromolecules* **1971**, *4*, 750.
    DOI: 10.1021/ma60024a016
37. Doi, M.; Edwards, S. F.The theory of Polymer Dynamics; Clarendon press: Oxford university press, **1986**.
    DOI: 10.1002/pol.1989.140270706
38. Saroj, M.; Bohidar, H. B. *Phys. Rev. E* **1998**, *58*, 729.
    DOI: 10.1103/PhysRevE.58.729